AIAA JOURNAL
Vol. 44, No. 9, September 2006

Parametric Two-Dimensional Finite Element Investigation: Shot Peening of High-Strength Steel

H. Lewis Zion*
Lockheed Martin Aeronautics Company, Marietta, Georgia 30063
and
W. Steven Johnson†
Georgia Institute of Technology, Atlanta, Georgia 30332-0405

DOI: 10.2514/1.19411

A parametric two-dimensional transient dynamic FEM is used to investigate the influence of two shot-peening specifications used on 4340M (300M) high-strength steel. One uses cast steel nominally 15% softer than the target, the other nominally 15% harder than the target. Details of the FEM development are provided. The FEM is then used for individual investigations carried out on the merits of the two shot specifications. A 2^4 factorial experimental design uses parametric variations of the FEM to detect the significance of shot diameter, velocity, target thickness and frictional coefficient on five response variables that include the following: the residual stress at the target surface and at the profile minimum, the depth corresponding to the minimum compressive residual stress, transition depth (near-surface compression to core tension) and the plastic work done on the target (percentage of initial kinetic energy). Deterministic linear models are generated for each response for both shot specifications using a completed factorial design approach. Probabilistic standard errors are estimated based on a normal distribution of the relative hardness between the shot and target using their yield strengths as an FEM proxy. The results demonstrate that the harder shot provides more beneficial material response within a tighter range.

Nomenclature

c	=	speed of sound
da/dN	=	rate of crack growth per cycle
E	=	modulus of elasticity
Et	=	tangent modulus
F	=	F statistic
H_A	=	alternate hypothesis
H_0	=	null hypothesis
P	=	probability
R^2	=	coefficient of determination
Rc	=	hardness (Rockwell c)
S–N	=	stress vs cycles to failure
X	=	random variable
α	=	stiffness damping factor or main effect coefficient
β	=	mass damping factor or 2-factor interaction coefficient
ΔK	=	stress intensity factor range
ε_u	=	strain to failure
μ	=	population mean or coefficient of friction
ν	=	Poisson ratio
σ	=	population standard deviation
σ_x	=	stress in the x direction (radial)
σ_y	=	stress in the y direction (normal)

I. Introduction

HIGH-STRENGTH steel is often the material of choice for structural components where the operating environment consists of infrequent applications of a very high limit load along with frequent applications of much lower amplitude fatigue loads. In these materials ductility as well as toughness must be compromised in order to meet the high yield strength requirement. Consequently, there is little capacity to sustain any appreciable stable crack growth before failure will occur. As such, single-load-path components of this type have had to be removed after a prescribed amount of flight time according to the safe-life philosophy. A prime example where this situation exists is in aircraft landing gear. Often shot peening is employed to improve the fatigue strength of these components through work hardening that causes a residual stress profile with a compressive layer at the surface which, in turn, serves to inhibit the initiation of cracks as well as arrest any inherent small cracks. This compressive layer also mitigates the deleterious effects of other undesirable surface damage (foreign object, corrosion, etc.). It is important that the compressive layer at the surface be of significant depth to contain the surface damage and thus preclude any of the variety of damage types from entering the region of (equilibrating) residual tension below. Obviously, this depth is controlled by the degree of work hardening that takes place.

The success of the shot-peening process, as measured by significant fatigue life improvement, depends on controlling key geometric and material parameters (e.g., shot size, hardness, velocity, etc.) in order to achieve a uniform residual stress profile throughout the surface of the component, particularly in regions of high stress. Historically, this has been achieved empirically by measuring the deflection of a standardized Almen strip subjected to the same intensity and length of exposure as the component being shot peened [1]. While this approach has provided a reasonable measure of quality assurance, the actual residual stress is seldom measured on the full-scale component. Moreover, because shot peening is a processing step, the potential exists for residual stress variation by virtue of the variance among the controlling parameters. As such, the benefits of shot peening have typically not been explicitly addressed as part of the material characterization phase of fatigue life prediction (i.e., coupon S–N and da/dN vs ΔK), though the benefit is usually present in the full-scale testing phase. Because very little attention has been paid to shot peening from an analytical perspective, a thorough understanding of both the mechanics of producing the residual stress profile (with specific interest in the work hardened layer of compression at the surface), as well as the potential for process variation, are seen as necessary steps toward the eventual development of better fatigue life prediction tools. These steps

Received 28 October 2005; revision received 11 April 2006; accepted for publication 11 April 2006.

*Damage Tolerance Engineer, C-141/C-5 Structural Engineering, Building B-27, 86 South Cobb Drive/Zone 0441.
†Professor, George W. Woodruff School of Mechanical Engineering.

coupled with parallel efforts toward improving the reliability of nondestructive inspection may eventually make high-strength steel components manageable using a damage tolerance approach.

With these thoughts in mind a two-dimensional (2-D) finite element investigation was conducted to determine how the residual stress state in a high-strength steel target varies in response to a single impact under a variety of scenarios with regard to process parameters. This effort builds upon the knowledge gained earlier in the investigation [2] where it was demonstrated that simulations of a single impact in 2-D provide considerable insight into the residual stress expectation associated with the shower of impacts seen in the actual shot-peening process. The sections that follow discuss the major elements of the investigation including process parameters considered, mathematical/statistical approach to predicting material responses, finite element modeling (FEM) approach and results along with a summary and conclusions.

II. Process Parameters Considered

A. Material Properties

The useful product of a single shot-peening impact event is the residual stress imparted by the particle to the target surface in the form of permanent plastic deformation (cold work). This plastic work is accomplished through the transformation of a portion of the initial kinetic energy of the particle. Under the best-case scenario the process is controlled in such a way that the target surface is not severely damaged while also allowing the particle to exit without incurring any permanent deformation. Obviously, the ability to meet this objective is highly dependent on the elastoplastic response of the two materials. For many engineering applications these objectives can be readily attained by using shot media that are significantly harder than the target. High-strength steel, thus, represents a somewhat unique shot-peened material due to its very high yield and ultimate strengths, thereby translating directly into a surface that is extremely hard. Because the surface is so hard it is difficult to impart a significant amount of compressive residual stress without incurring, at least, some permanent shot deformation.

Given these observations, one parameter that must be included in an investigation of this type is the relative hardness of the shot compared with the target. In this regard, two shot specifications (Mil S 13165B and SAE J827) that have been used by the aircraft industry to shot peen 4340M (300M) high-strength steel were considered. The first uses cast steel shot media that are nominally 15% harder than the target, whereas the other uses cast steel shot media that are approximately 15% softer than the target. These two specifications formed the basis of a coupon test program conducted in the Materials Processing Research Laboratory (MPRL) at Georgia Institute of Technology that was part of an investigation privately funded by Delta Air Lines. Those experimental results generally demonstrated that 300M specimens peened with the harder shot had better fatigue resistance than with the softer shot, though there was some overlap in the two scatter bands. The hardness, ultimate tensile strength (UTS) and yield strength (YS) of the target and two shot materials are listed in Table 1. The shot hardnesses shown in bold represent the range allowed by the respective specifications. In the case of the target, the ranges of the yield and ultimate strengths are shown in bold rather than the hardness. The relationship between hardness and ultimate tensile strength provided in Dowling [3] is used to derive the UTS range for the shot and hardness range for the target. The lower yield strength of the target comes from the 300M value listed in [4] with approximately the same nominal UTS whereas the higher yield strength comes from the corresponding listing in [5].

Table 1 illustrates that there is a significant amount of possible yield strength variation between shot and target when either one of the two peening specifications is used. For the purpose of this investigation it is both reasonable and convenient to assume that the yield strength of the target and particular peening media are normally distributed within a $\pm 3\sigma$ (i.e., ± 3 standard deviations) range that encompasses the range of values listed. This assumption enables the two respective yield strengths (target and either *hard* or *soft* shot particle) to be combined into a single normal random variable, Rel-YS, according to the following:

$$\text{Rel}-\text{YS} = \frac{X - (\mu_{\text{ys}}^{\text{shot}} - \mu_{\text{ys}}^{\text{targ}})}{[(\sigma_{\text{ys}}^{\text{shot}})^2 + (\sigma_{\text{ys}}^{\text{targ}})^2]^{1/2}} \tag{1}$$

where the $\boldsymbol{X}$ denotes the difference between the actual yield strength of the particular shot particle and the 300M target. Here, the relative yield strength (Rel-YS), rather than relative hardness is used, because it is tractable from an FEM perspective. The yield strengths have been assigned according to a fixed percentage of ultimate strength, which has a direct linear relationship to hardness.

Having established Rel-YS as a probabilistic parameter given the stochastic nature of ultimate tensile strength (UTS) by virtue of hardness, the remaining material properties necessary to conduct the investigation were treated deterministically. These included E, ν, and ε_u. Additionally, an elastic-linear-hardening constitutive relationship was assumed for the target and soft shot whereas the hard shot was assumed to be elastic-perfectly plastic. These additional mechanical properties are listed in Table 2.

B. Geometric Properties

In addition to the material variation described above, several geometric parameters involved in the process were also considered in this investigation. These included shot diameter, shot velocity, target

Table 1 Shot and target basic material properties

					Shot specifications					
Spec ID:	Mil-S-13165B									
Material	Hardness range (Rc)		UTS (Ksi)		UTS (MPa)		YS estimate (Ksi)		YS estimate (MPa)	
Cast steel	Low	High	Low	High	Low	High	Low	High	Low	High
	55	**65**	314	403	2165	2779	298	383	2057	2641
	Nominal	60	Nominal	359	Nominal	2472	Nominal	341	Nominal	2349
								Yield strength assumed 95% of UTS		
Spec ID:	SAE J827									
Material	Hardness range (Rc)		UTS (Ksi)		UTS (MPa)		YS estimate (Ksi)		YS estimate (MPa)	
Cast steel	Low	High	Low	High	Low	High	Low	High	Low	High
	40	**50**	180	270	1244	1858	153	229	1057	1580
	Nominal	45	Nominal	225	Nominal	1551	Nominal	191	Nominal	1319
								Yield strength assumed 85% of UTS		
					Target specification					
Spec ID:	AMS 6257/6419									
Material	Hardness range (Rc)		UTS (Ksi)		UTS (MPa)		YS actual (Ksi)		YS actual (MPa)	
300M	Low	High	Low	High	Low	High	Low	High	Low	High
	50.6	53.4	**275**	**300**	1896	2069	**230**	**245**	1586	1689
	Nominal	52.0	Nominal	288	Nominal	1982	Nominal	238	Nominal	1638

Table 2 Additional shot and target mechanical properties

Shot						
Mil-S-13165B						
ε_u (%)	E (Msi)	ν	Et estimate (Ksi)[a]		Et estimate (MPa)[a]	
Nominal	Nominal	Nominal	Nominal		Nominal	
1	30	0.28	0		0	
SAE J827						
ε_u%	E (Msi)	ν	Et estimate (Ksi)		Et estimate (MPa)	
Nominal	Nominal	Nominal	Low	High	Low	High
5	30	0.28	603	954	4157	6580
			Nominal	779	Nominal	5369
Target						
AMS 6257/6419						
ε_u %	E (Msi)	ν	Et estimate (Ksi)		Et estimate (MPa)	
Nominal	Nominal	Nominal	Low	High	Low	High
7	29	0.32	725	894	4999	6161
			Nominal	809	Nominal	5580

[a]Assumed perfectly plastic at YS.

Table 3 Contrasting values for geometric parameters

Parameter	Low level (−1)	High level (+1)
Shot diameter	0.72 mm (0.028 ins)	1.08 mm (0.043 ins)
Shot velocity	50 mps	75 mps
Target thickness	1.44 mm (0.056 ins)	2.88 mm (0.112 ins)
Frictional coefficient	0	0.5

thickness, and whether or not contact friction was present. For each of these parameters two contrasting nominal values were considered based on the residual stress response variables being measured. Since each of these parameters can be fairly well controlled, there was no attempt made to consider statistical variation around these nominal values. A summary of the contrasting *high* and *low* values assigned to each geometric parameter is provided in Table 3. These high and low levels were applied to both of the (nominal) shot hardness values from Table 2. Henceforth it is implied that "−1" and "+1" refer to the assigned *end points* listed in Table 3. The method of assessing the effect of various combinations of these four parameters on five key response variables, under a scenario involving nominal material properties of either the soft (Rc45) or hard (Rc60) shot impacting a 300M target, will now be discussed.

III. Mathematical/Statistical Approach to Predicting Material Responses

Five key material residual stress response metrics were identified in this investigation. These included the following: 1) residual stress (σ_x) at the target surface, 2) residual stress (σ_x) at the profile minimum, 3) depth corresponding to the profile minimum residual stress (σ_x), 4) depth at the core transition from compression to tension, and 5) plastic work done on the target as a percentage of the original shot kinetic energy. To assess the impact of the four key process parameters (shot diameter, velocity, target thickness, and presence of frictional coefficient) on these various response variables a variation of the *design of experiments* (DOE) statistical procedure, commonly used to facilitate quality control, was employed. This procedure used analysis of variance (ANOVA) to establish the relative influence of the suspect process variables as well as interactions among them, on the five responses of interest. Use of this approach resulted in a 2^4 *full factorial* experimental design involving the variables listed in Table 3 at each of the two hardness values. For purposes of discussion, these designs are designated as runs 1 through 16 for the nominal Rc45 shot and runs 17 through 32 for the nominal Rc60 shot as presented in Table 4.

An important property of this design arrangement is that the combinations of factors are deliberately arranged in what is known as an *orthogonal array*. Specifically, the dot product of any column or product of columns with another column produces a zero result,

Table 4 2^4 factorial design arrangement for two shot hardnesses

Rc45 run	Rc60 run	Diameter	Velocity	Thickness	Friction
1	17	−1	−1	−1	−1
2	18	+1	−1	−1	−1
3	19	−1	+1	−1	−1
4	20	+1	+1	−1	−1
5	21	−1	−1	+1	−1
6	22	+1	−1	+1	−1
7	23	−1	+1	+1	−1
8	24	+1	+1	+1	−1
9	25	−1	−1	−1	+1
10	26	+1	−1	−1	+1
11	27	−1	+1	−1	+1
12	28	+1	+1	−1	+1
13	29	−1	−1	+1	+1
14	30	+1	−1	+1	+1
15	31	−1	+1	+1	+1
16	32	+1	+1	+1	+1

thereby making them orthogonal in vector space. This enables the investigator to determine, not only the significance of the individual factors (commonly referred to as *main effects*), but also the level of significance of interactions among these factors. The means of achieving these ends will become clearer when the results are discussed, however, expanded discussion of the theoretical underpinnings of ANOVA models in general, and factorial designs in particular, is available in [6]. The basic approach will be to generate a mathematical representation for each of the five response variables that consists of a set of deterministic coefficients that account for the main effects and interactions present within the process space encompassed by the ranges listed in Table 3, plus a stochastic component to be mapped from the relative hardness variable defined in Eq. (1). These mathematical models will be generated at both nominal hardness values. Again, the specific details that went into formulating these models will become clearer when the results are discussed. However, before doing so a brief overview of the FEM approach used to generate the data is in order.

IV. Finite Element Modeling Approach

A. Model Formulation

The FEM procedure used in this investigation was mainly developed in an earlier investigation that used the ANSYS® (registered trademark of ANSYS, Inc.) finite element code as a means of predicting results generated in a published experimental investigation involving a medium steel target being impacted by a ball bearing dropped onto its surface [7]. The basic restrained axisymmetric two-dimensional (2-D) model is depicted in Fig. 1. It uses 8-noded 2-D solid elements (with the axisymmetry option invoked) and surface-to-surface element pairings that detect the

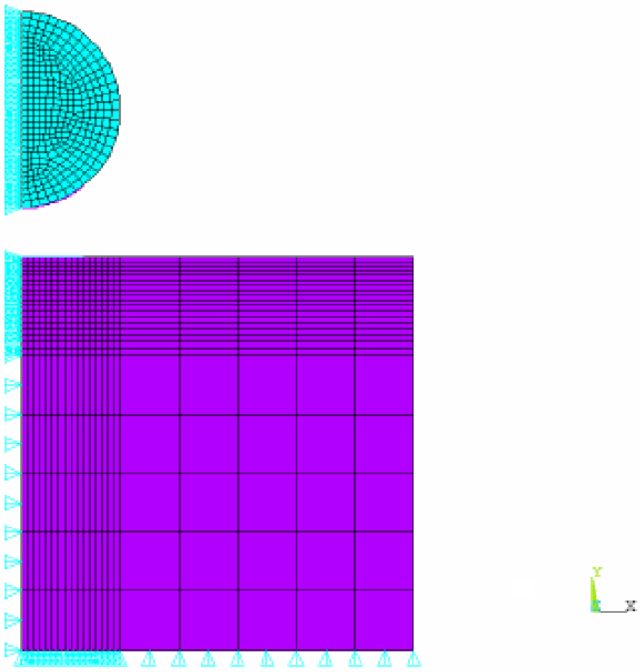

Fig. 1 Restrained axisymmetric 2-D model.

presence of contact between surfaces on the shot particle and stationary target. A given surface-to-surface element pairing consists of two three-noded surface elements; one is designated as the target surface, whereas the other is designated as the contact surface. Elastic action of the two surfaces relative to one another is dictated through a shared set of constants. In this way a given surface, designated as a target, can have multiple contact surfaces associated with it. The choice of which surface to designate as the target is dictated by the particular aspects of the problem. In this investigation it was convenient to locate the target (not to be confused with the physical target end of the cylinder) surfaces on the moving particle and the contact surfaces on the stationary surface of the cylinder. The stationary cylindrical target material is restrained along its base to act as a rigid foundation, whereas both the target and particle are restrained along the centerline axis of symmetry. A cylindrical coordinate system is shown in Fig. 1, where the *X–Z plane* is actually the *R–θ plane* in cylindrical space and the *Y axis* represents the axis of the cylinder. In addition to the static boundary conditions displayed in the figure, a kinematic boundary condition comprising an initial velocity had to be applied to the particle. This was accomplished by moving the particle through one time step with a given displacement occurring in a specified period of time.

B. Model Solution and Optimization

In general, a given solution sequence proceeds by direct integration of small time steps with dynamic equilibrium satisfied at each within a small convergence error. Practical implementation thus requires that the time derivatives (in the equations of equilibrium) be approximated by means of finite time differences (i.e., linear differences for velocity, squared differences for acceleration). Solution algorithms suited to this task are broadly categorized as either explicit or implicit. A detailed discussion of the two approaches is provided in Cook et al. [8]. ANSYS specifically employs a Newmark time integration scheme that can operate either implicitly or explicitly depending on the material damping parameters chosen by the user (note that if no damping parameters are chosen by the user the solution will proceed explicitly). Given the constraints of this investigation it was decided early on to use an implicit solution. This decision was justified by the assumption that any dynamic response that would take place within the material in the form of stress wave propagation would not play a significant role in creating the residual stress state. Specifically, the impact causes very low amplitude, high frequency acoustical stress waves to occur in the material that do not significantly affect the outcome, but nonetheless require an extremely small time step in order to provide stability in an explicit solution. This numerical phenomenon arises from the need to track the stress wave propagation, at a frequency consistent with c, across the small element size necessary for accurate prediction of stresses in the localized area of the impact. Given that elements with quadratic sides are being used, the required time step under such a scenario would be approximately half the smallest free edge of one of the solid elements divided by the speed of sound in the material. This would lead to an extremely long solution time to the point of being impractical.

As a result of the aforementioned considerations, the choice was made to use a stable implicit Newmark solution of second-order accuracy. The implicit solution was achieved through the inclusion of a β factor of 0.25. The accompanying α was assigned a value of zero given the very small amount of structural damping present in the materials being considered. It is worth noting that the α and β notation in the ANSYS code is reversed from Cook et al. [8] (i.e., α is mass damping and is β stiffness damping). This method of implicit solution offers the advantages of no numerical damping with unconditional stability (i.e., is independent of time step size). However, it is important to note that accuracy improves as the size of the time step is reduced according to the trapezoidal rule. By default ANSYS uses a global 0.5% error in force (and moment) equilibrium at a given time step as its primary convergence criteria along with a secondary criteria of 0.5% error in displacement [9]. These values were not altered for this investigation.

Two load (applied in terms of elapsed time) steps were used to encompass the full impact transient. The first step established the initial particle velocity as already discussed. The second step covered the actual impact transient encompassed by the time taken to completely decelerate from its initial surface penetration, begin to reaccelerate in the opposite direction and completely exit with a fraction of its initial kinetic energy. The time expenditure for this second step was 10 μs in the vast majority of cases, however, in cases where the softer shot had an initial velocity of 75 mps the time size of the second time step had to be lengthened to 15 μs to enable the particle to complete its exit. To run in the background (batch) mode the upper bound on the number of allowable equilibrium iterations per time substep was increased to 200 from the default value of 25. This did not affect the solution time (the number of iterations varies to the extent necessary to meet the convergence criteria); however, it did avoid the necessity for intermediate restarts.

An examination of Fig. 1 reveals a region of contact in the upper left-hand corner of the target. Keeping in mind that this region is actually cylindrical in physical (three-dimensional) space, it was important to obtain the level of mesh refinement necessary to properly map the residual stress gradient left in the material following the impact transient. Given the localized area of plastic deformation within this region, the number of elements in both the radial and depth directions was varied along with the radial and depth dimensions until mesh convergence was achieved. The criterion for mesh convergence was one in which there was close agreement between the element and nodal stresses; the latter being a nodal average of the former. In addition, the size of the region of contact was scaled up, to the extent necessary, in cases involving the larger particle diameter, while adhering to the aforementioned convergence criterion. An illustration of this procedure is presented for selected cases along with the results that follow.

V. Results

As illustrated in Table 4, a 2^4 factorial design was constructed to measure the effects of varying the diameter, velocity, thickness, and friction on five residual stress response metrics. Additionally, the stochastic effect of the relative hardness by virtue of the relative yield strength (Rel-YS) of the soft (Rc45) or hard (Rc60) shot relative to its 300M target, was also included. The end result was a linear combination of deterministic coefficients with respect to the range of variability considered in the factorial design plus an additional

probabilistic term derived from the Rel-YS investigation. Since, the results differ markedly with regard to nominal shot hardness it is convenient to consider them separately.

A. Rc45 Impact Study

A comparison between the nodal and element (x direction) residual stress (σ_x) results at the completion of the transient for run 1 (i.e., parametric values of 0.72 mm shot diameter, 50 mps velocity, 1.44 mm thickness, and $\mu = 0$) is provided in Fig. 2. The fact that there is good agreement between the nodal residual stress contours on the left which are averages of the nearest neighbor element stresses on the right indicates that good mesh convergence has been achieved. This mesh convergence check was performed for all the simulations performed throughout this investigation. The target residual stress (σ_x) profile for run 1 is provided in Fig. 3. This profile measures the radial component of residual stress (parallel to the surface) of the target at the bottom of the dent in the direction of penetration (i.e., along the Y axis of radial symmetry; X and Z both equal to zero) extending in the material depth direction. It is interesting to note that there is residual tension at the base of the dent that transitions to compression approximately 0.020 mm below the dent surface. The residual stress then remains compressive until approximately 0.179 mm below the surface where it transitions to tension in the core region. This *puddle* of tensile material can clearly be seen in Fig. 2. It is also worth noting that the shot particle has plastically deformed after impact and been left with a flattened edge due to its lower yield strength in relation to the target surface.

The residual stress profiles for the other 15 cases in the factorial design were also obtained, as was the amount of plastic work done, expressed as a percentage of the original particle kinetic energy, on the target for all cases. The actual particle kinetic energy for each run is summarized in Table 5 so that the percentages in Table 6 and later in Table 10 may be converted to actual kinetic energy if desired. The complete set of response data is provided in Table 6. In addition to the quantitative summary in Table 6, the residual stress (σ_x) profiles for all 16 of the Rc45 runs (i.e., runs 1 through 16, where cases of similar behavior have been combined) are presented in Fig. 4. A review of these results finds significant variability among the combinations of variables. There are several algorithms for measuring the significance of the main effects and interactions contained within this 2^4 factorial design. These techniques fall under the heading of generalized linear models (GLMs) within the broader category of analysis of variance (ANOVA) statistical methods. Here, the term statistical is somewhat misleading because the finite element models

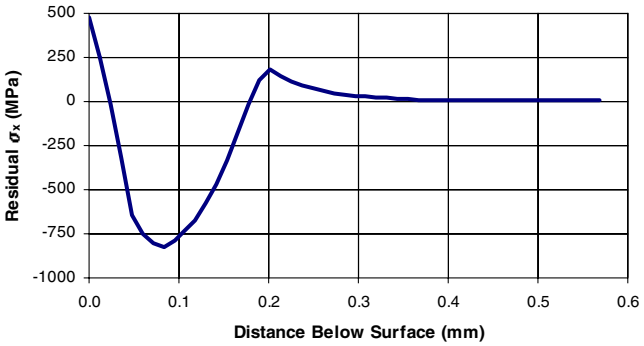

Fig. 3 Target residual stress (σ_x) profile for run 1.

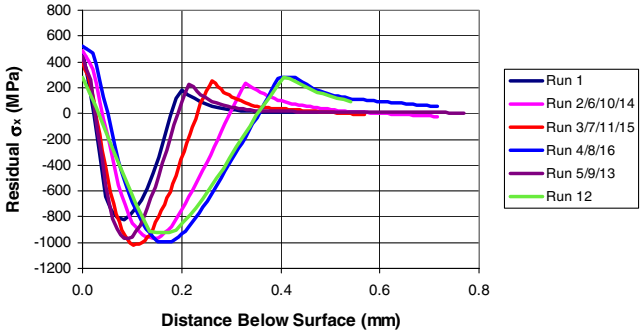

Fig. 4 Residual stress (σ_x) summary for Rc45 runs.

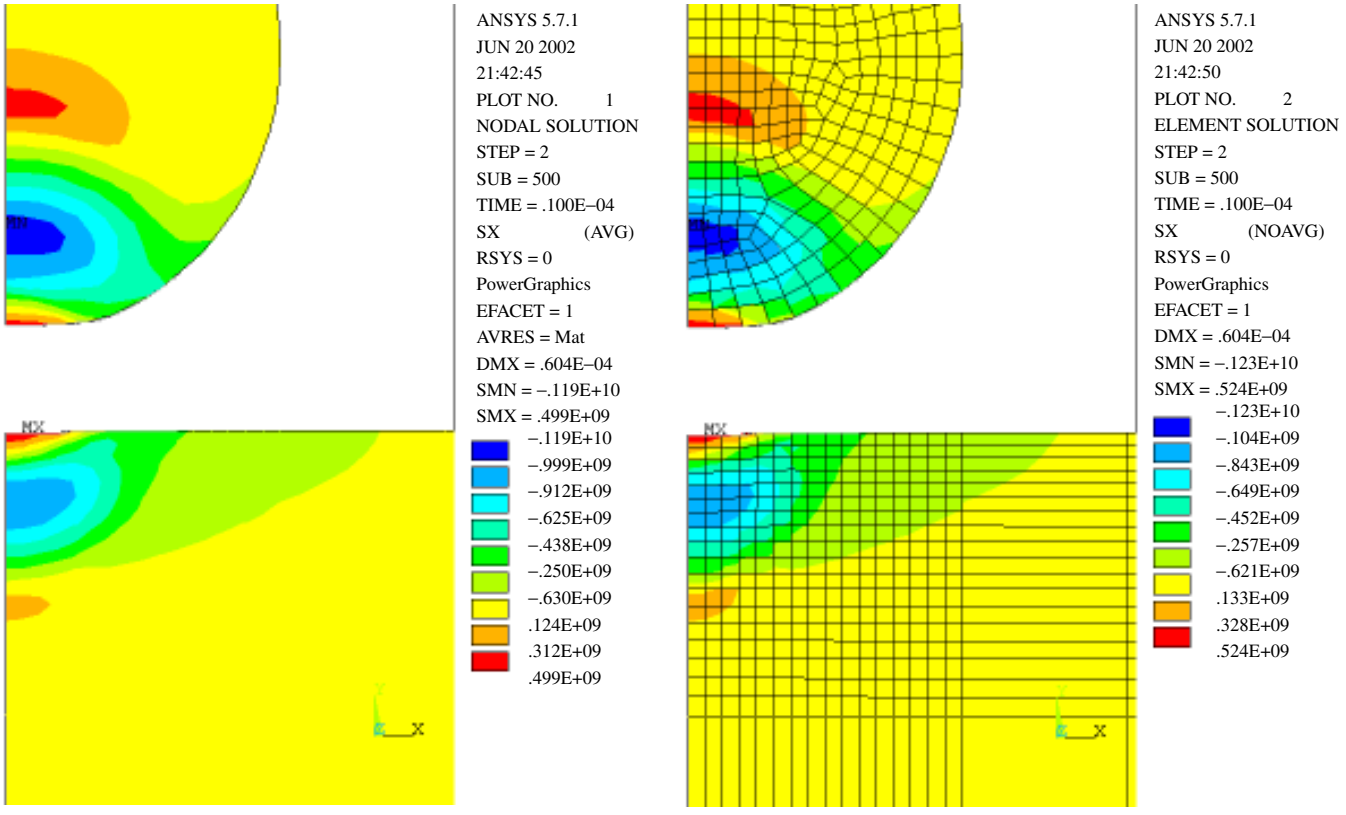

Fig. 2 Comparison of nodal and element residual stress (σ_x) results in pascals for run 1.

used to generate the data are deterministic (i.e., the resultant responses are invariant for each combination of variables). Notwithstanding, the ANOVA approach provides a means of culling the important main effects and interactions affecting the measured responses of interest. In this case the assumption was made that a GLM containing the four main effects and six 2-factor interaction terms would be adequate to linearize the data. Under the assumed model the remaining 3-factor and 4-factor interaction terms along with their 5 degrees of freedom (DF) are used as a source of *pseudo* residual error with which to estimate the significance of the main effects and 2-factor interaction terms.

In order to facilitate the ANOVA, the Minitab® (registered trademark of Minitab, Inc.) statistical software package was used. The surface residual stress (σ_x) ANOVA result for the aforementioned GLM (main effects and 2-factor interactions) is presented in Table 7. Here, the term source in the first column refers to the particular main effect or 2-factor interaction being tested for significance. The 2-factor interactions in Table 7 and 8 (and Table 10 and 11 for the Rc60 results) are listed as a product of the particular main effects that are interacting with one another (e.g., diameter ∗ velocity or diameter × velocity). Each of these sources has a single DF attributable to the mean response within its member group comprising responses with the same attribute setting. That particular group mean response is subtracted from the individual response of all of the group constituents and the squared deviations summed to get its within-group sum-of-squares (SS). The mean square (MS) of each group is simply its SS divided by its DF. An F statistic is computed for each of the source effects by comparing its MS to the mean square error (MSE). P is obtained by comparing the particular F statistic to the computed value with 1 DF in the numerator and 5 DF in the denominator. It is the probability of accepting the null hypothesis that the coefficient associated with the source is zero (i.e., the particular source has no effect on the response). A low P value implies that H_0 should be rejected in favor of the H_A; namely, that the coefficient associated with the source is nonzero and thus, significant to the GLM. As a rule of thumb for this investigation, sources with P values less than 0.1 (10%) were considered highly significant. On that basis, friction ($P = 0.033$) is the only highly significant main effect and there are no other significant main effects or interactions.

Because the aim of the GLM is to generate a linear representation of the data, a summation of coefficients for each source was generated and the fitted line, comprising all the coefficients (i.e., from all four main effects plus the six 2-factor interactions, even though not all have been deemed significant) along with the overall average, compared with the actual responses. As such, highly significant sources result in coefficients with much higher magnitude and thus, have more influence on the predicted outcome, than those that are less significant. The actual-vs-fit and fit-line prediction for the surface residual stress (σ_x) are depicted in Fig. 5. This figure shows that the chosen GLM, comprising main effects and 2-factor interactions, has a fairly good predictive quality. A quantitative measure of the fit quality can be obtained from the coefficient of simple determination, R^2 as calculated by comparing the explained variation (i.e., the total SS minus the error SS) to the overall variation (total SS); in this case R^2 is 89.8%. Note that, because the 3 and 4-factor interactions were pooled to construct the (pseudo) error SS, a perfect fit would have been attainable had they been included in the GLM. However, no quantitative measure of the significance of the effects could have been calculated without a mean square error (MSE) source, though there are qualitative plotting procedures for determining significant main effects and interactions as detailed in Box et al. [10].

The *surface residual stress* (σ_x) fit in Fig. 5 is symbolically represented by the following expression:

$$\hat{y}_i = \bar{y} + \alpha_1 x_{1i} + \alpha_2 x_{2i} + \alpha_3 x_{3i} + \alpha_4 x_{4i} + \beta_{12} x_{1i} x_{2i} + \beta_{13} x_{1i} x_{3i} + \beta_{14} x_{1i} x_{4i} + \beta_{23} x_{2i} x_{3i} + \beta_{24} x_{2i} x_{3i} + \beta_{34} x_{3i} x_{4i} \quad (2)$$

where the α's and β's (not to be confused with the stiffness and mass damping factors introduced earlier) are the main effect and 2-factor interaction coefficients, respectively. Again, unlike a conventional ANOVA model where residual error is stochastic, in the procedure used herein it is deterministic, having been deliberately generated from the 3 and 4-factor interactions gathered in numerical FEM

Table 5 Initial kinetic energy summary

	Runs			
Rc45 shot	1, 5, 9,13	2, 6,10,14	3, 7,11,15	4, 8,12,16
Rc60 shot	17,21,25,29	18,22,26,30	19,23,27,31	20,24,28,32
Initial K.E. (Joules)	1.85E-03	6.46E-03	4.15E-03	1.45E-02

Table 7 ANOVA results for residual stress (σ_x) at the surface

Source	DF	SS	MS	F	P
Diameter	1	15,563	15,563	2.97	0.145
Velocity	1	11,936	11,936	2.28	0.191
Thick	1	10,151	10,151	1.94	0.223
Friction	1	44,627	44,627	8.53	0.033
Diameter ∗ Velocity	1	4,935	4,935	0.94	0.376
Diameter ∗ Thick	1	9,555	9,555	1.83	0.235
Diameter ∗ Friction	1	4,064	4,064	0.78	0.419
	1	3,511	3,511	0.67	0.450
Velocity ∗ Friction	1	518	518	0.10	0.766
Thick ∗ Friction	1	116	116	0.02	0.888
Error	5	2,6171	5,234		
Total	15	131,144			

Table 6 Complete set of response data for Rc45 shot

Run ID	Diameter	Velocity	Thickness	Friction	σ_x at surf (MPa)	σ_x min (MPa)	Depth at min (mm)	Trans depth (mm)	Plastic work percent of original K.E.
1	−1	−1	−1	−1	475	−825	0.083	0.178	8.67%
2	+1	−1	−1	−1	487	−968	0.150	0.290	12.55%
3	−1	+1	−1	−1	403	−1018	0.102	0.231	12.68%
4	+1	+1	−1	−1	524	−997	0.179	0.355	11.10%
5	−1	−1	+1	−1	442	−969	0.085	0.192	14.87%
6	+1	−1	+1	−1	460	−977	0.137	0.292	13.73%
7	−1	+1	+1	−1	269	−1058	0.116	0.235	10.73%
8	+1	+1	+1	−1	495	−992	0.162	0.350	12.03%
9	−1	−1	−1	+1	349	−982	0.097	0.193	14.26%
10	+1	−1	−1	+1	406	−969	0.150	0.296	12.60%
11	−1	+1	−1	+1	413	−999	0.114	0.232	12.43%
12	+1	+1	−1	+1	277	−923	0.149	0.354	12.28%
13	−1	−1	+1	+1	355	−963	0.085	0.192	12.10%
14	+1	−1	+1	+1	377	−978	0.137	0.292	13.80%
15	−1	+1	+1	+1	177	−1046	0.116	0.235	10.82%
16	+1	+1	+1	+1	356	−977	0.162	0.350	12.13%

Table 8 Summary of GLM coefficients, significance, and fit quality with Rc45 shot

		Main effects				Interactions						
Response	Mean	Diameter	Velocity	Thick	Friction	Diameter × Velocity	Diameter × Thick	Diameter × Friction	Velocity × Thick	Velocity × Friction	Thick × Friction	ANOVA R^2
σ_x at surf (MPa)	391.56	−31.19	27.31	25.19	52.81	17.56	24.44	−15.94	−14.81	−5.69	2.69	89.8%
σ_x min (MPa)	−977.50	−4.88	23.75	17.50	2.13	24.13	9.13	13.00	0.50	17.13	6.13	89.9%
Depth at min (mm)	0.1265	−0.0268	−0.0110	0.0015	0.0003	−0.0013	−0.0023	−0.0035	0.0030	−0.0020	0.0003	98.7%
Trans depth (mm)	0.2667	−0.0557	−0.0261	−0.0006	−0.0013	0.0038	−0.0019	−0.0007	−0.0008	−0.0013	−0.0013	99.9%
Plastic work (% of lnit K.E.)	12.23	−0.1615	0.5911	−0.2974	−0.1868	−0.1864	0.2354	−0.1478	−0.5078	−0.1819	−0.4994	71.9%

Table 9 Response data and fit quality for Rc45-300M stochastic Rel-YS simulations

Std normal Z score	Rel YS (MPa)	σ_x at surf (MPa)	σ_x min (MPa)	Depth at min (mm)	Trans depth (mm)	Plastic work percent of original K.E.
−2.5	−541	283	−692	0.085	0.170	7.39%
−1.25	−430	288	−847	0.085	0.182	10.54%
0	−319	349	−982	0.097	0.193	14.26%
1.25	−208	358	−1116	0.097	0.202	18.61%
2.5	−97	380	−1269	0.097	0.210	23.40%
Normal dist R^2		91.44%	99.92%	74.90%	99.20%	99.33%
Std error estimate		19.4	115.4	N.A.	0.008	3.20%

simulations. This deterministic linearization is appropriate given that the diameter, velocity, and target thickness can be controlled to fairly tight tolerances with respect to their nominal target values. The other main effect of friction is a little more abstract in that it is not deliberately controlled to a nominal value; however, it was noted here as well as in a previous investigation that the frictional effect is constant once a *no-slip* condition is established. Specifically, once significant deformation occurs the normal force insures that the friction will not be overcome.

A summary of the 10 GLM coefficients (with Rc45 Shot) associated with all five response variables is provided in Table 8 along with the particular fit quality of each per its R^2 value. Those coefficients associated with highly significant ANOVA sources (i.e., with P values <0.1) are shaded. The procedure for obtaining the coefficients is detailed in Box et al. [11]. To generate a prediction for a particular Table 6 result using these coefficients, one must use the sign associated with the given main effect while generating the appropriate sign for the particular interaction term based on the signs of its two associated main effects (e.g., for run 1 the diameter × velocity interaction would take on a +1, given the product of the two negative signs). The Table 8 results show that the adopted GLM, comprising main effects and 2-factor interactions, does a reasonably good job of predicting the residual stress (σ_x) at the surface and the residual stress (σ_x) minimum, and an excellent job of predicting the depth at the minimum residual stress (σ_x) and the transition depth. In contrast, the GLM does a relatively poor job of predicting the plastic work percentage. These observations will be elaborated upon following the discussion of the Rc60 results.

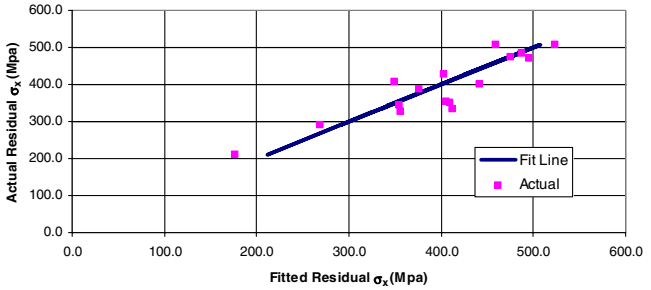

Fig. 5 Actual-vs-fit and fit-line prediction for *surface residual stress* (σ_x).

Earlier it was noted that the relative hardness between the shot and target material constitutes a probabilistic effect on residual stress state response. In the case of the surface residual stress (σ_x), the response will vary depending on where the hardness values of the shot and target materials occur within their respective hardness (tolerance) bands. Therefore, it is appropriate to add a probabilistic term to the predictive models summarized in Table 8. In pursuit of this goal, a series of four FEM simulations were conducted where the geometric parameters were held constant (0.72-mm shot diameter at 50-mps velocity with a 1.44-mm thick target and a frictional main effects interactions coefficient of 0.5), whereas the relative yield strength (Rel-YS), defined in Eq. (1), was varied using the ranges of Rc45 shot and 300M target material data contained in Table 1. In performing these simulations the Rel-YS was assigned standard normal (Z) scores of 2.5, 1.25, 1.25, and 2.5. The tangent moduli were held to the nominal values listed in Table 2 throughout. The five residual stress state responses as a function of Rel-YS Z-score (i.e., standard normal score or number of standard deviations from the mean), including the nominal results from run number 9 from Table 6 (i.e., $Z = 0$, Rel–YS $= -319$ MPa), are provided in Table 9 along with a normal distribution coefficient of simple determination (R^2).

The results in Table 9 indicate that a probabilistic term, based on a normal distribution of relative yield strength, is an excellent approximation, by virtue of the R^2 value, for the minimum residual stress (σ_x), transition depth and plastic work percentage and a reasonably good approximation for the surface residual stress (σ_x). In the case of the depth at the minimum residual stress (σ_x), it is a poor approximation (as there are only two values among the five Z scores). The standard error (SE) estimates in the table were generated by taking the absolute value of the range of the particular response and dividing by five. The SE estimates in Table 9 are intended to account for stochastic material variation in light of the mean responses provided in Table 6 and also provide realistic error bands for predictions made from coefficients in Table 8.

B. Rc60 Impact Study

The results for the hard (Rc60) shot were generated analogously to those for the soft (Rc45) shot. As such, a comparison between the

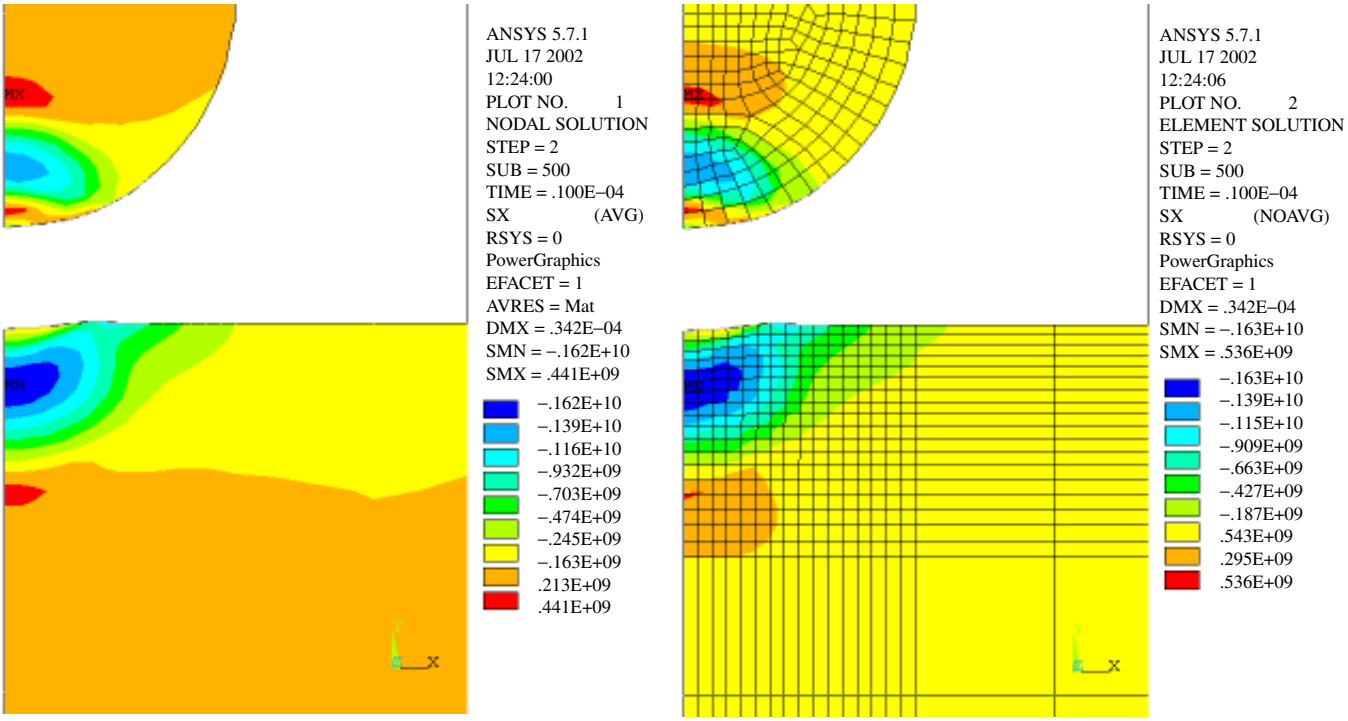

Fig. 6 Comparison of nodal and element residual stress (σ_x) results in pascals for run 17.

nodal and element residual stress (σ_x) results at the completion of the transient for run 17 (i.e., parametric values of 0.72-mm shot diameter, 50-mps velocity, 1.44-mm thickness, and $\mu = 0$) is provided in Fig. 6 along with its associated target residual stress (σ_x) profile at the bottom of the dent along the *Y axis* of radial symmetry in Fig. 7. These figures illustrate that, for the same set of variables, the hard shot produces residual compression at the surface instead of the puddle of tension that the soft shot produced (as seen in Figs. 2 and 3). In addition the magnitude of the minimum compressive residual stress (σ_x) and its associated depth are significantly greater and a noticeable dent and rounded shot surface have replaced the shallow dent and flattened shot seen earlier.

Table 10 provides the complete set of response data for the Rc60 shot. A comparison of these values with the analogous Rc45 shot responses in Table 6 immediately brings out the fact that, on average, the Rc60 shot produces a much higher magnitude of compressive residual stress that extends deeper into the subsurface region. In addition, there is roughly a fourfold increase in the percentage of plastic work converted from the initial kinetic energy of the particle. These findings can be explained by the physics of the shot impingement. Namely, because the Rc60 shot is 15% harder than the target (vs 15% softer for the Rc45 shot), it is able to convert significantly more of its kinetic energy into target plastic work and produce a greater depth and magnitude of compressive residual stress.

Whereas, there was tension at the base of the dent for all cases with the Rc45 shot, the Rc60 shot only produces this condition when friction is present. Other comparisons will be made when the overall summary and conclusions are presented at the end of the paper. In addition to the quantitative summary in Table 10, the residual stress (σ_x) profiles for all 16 of the Rc60 runs (i.e., runs 17 through 32, where cases of similar behavior have been combined) are presented in Fig. 8. In general, all the profiles show a smooth transition of residual stress throughout the range of depth presented, however, some of the cases involving friction (i.e., even-numbered runs) show some slight degree of kinkiness in the first 0.2 mm.

Table 11 provides the analogous GLM coefficient, significance identification and fit quality for the hard shot as was presented for the soft shot in Table 8. These Rc60 results demonstrate excellent fit quality in all cases as well as a more dominant character of the

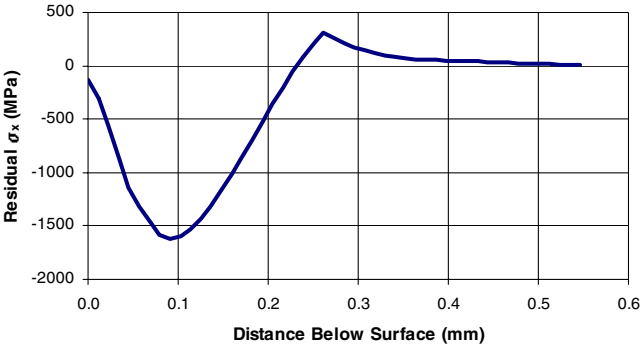

Fig. 7 Target residual stress (σ_x) profile for run 17.

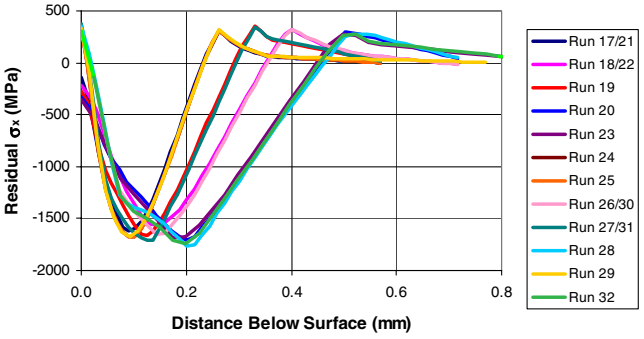

Fig. 8 Residual stress (σ_x) profile summary for Rc60 runs.

constituent main effects to map the responses when compared with the earlier Rc45 results. The probabilistic standard error and fit quality, analogous to the Rc45 300M Rel-YS presented in Table 9, has been generated for the Rc60 300M Rel-YS in Table 12. These results show that the normal distribution is an excellent approximation for all but the depth at the minimum residual stress (σ_x). While a comparison of the two sets of results finds general agreement, the Rc60 shot produces a better fit to the surface residual stress (σ_x) than the analogous Rc45 result. Additionally, with the

Table 10 Complete set of response data for Rc60 shot

Run ID	Diameter	Velocity	Thickness	Friction	σ_x at Surf (MPa)	σ_x min (MPa)	Depth at min (mm)	Trans depth (mm)	Plastic work percent of original K.E.
17	−1	−1	−1	−1	−134	−1615	0.091	0.232	47.44%
18	+1	−1	−1	−1	−217	−1565	0.143	0.351	44.65%
19	−1	+1	−1	−1	−271	−1664	0.125	0.291	48.58%
20	+1	+1	−1	−1	−327	−1711	0.201	0.455	45.87%
21	−1	−1	+1	−1	−132	−1600	0.092	0.216	44.76%
22	+1	−1	+1	−1	−122	−1549	0.149	0.348	46.89%
23	−1	+1	+1	−1	−266	−1718	0.123	0.295	45.48%
24	+1	+1	+1	−1	−349	−1681	0.174	0.448	46.54%
25	−1	−1	−1	+1	337	−1680	0.102	0.234	46.95%
26	+1	−1	−1	+1	281	−1647	0.143	0.354	44.08%
27	−1	+1	−1	+1	378	−1713	0.137	0.295	47.44%
28	+1	+1	−1	+1	349	−1763	0.201	0.463	44.81%
29	−1	−1	+1	+1	334	−1677	0.092	0.234	44.25%
30	+1	−1	+1	+1	367	−1629	0.149	0.351	46.34%
31	−1	+1	+1	+1	422	−1770	0.123	0.298	44.34%
32	+1	+1	+1	+1	311	−1746	0.199	0.454	46.94%

Table 11 Summary of GLM coefficients, significance, and fit quality with Rc60 shot

		Main effects				Interactions						
Response	Mean	Diameter	Velocity	Thick	Friction	Diameter × Velocity	Diameter × Thick	Diameter × Friction	Velocity × Thick	Velocity × Friction	Thick × Friction	ANOVA R^2
σ_x at surf (MPa)	60.06	23.44	29.19	−10.56	−287.31	−11.44	4.56	3.06	−11.94	46.81	0.56	99.6%
σ_x min (MPa)	−1670.50	−9.13	50.25	0.75	32.63	−13.63	10.88	−2.25	−7.25	5.38	−1.63	98.0%
Depth at min (mm)	0.1403	−0.0296	−0.0201	0.0026	−0.0030	0.0038	0.0005	0.0001	−0.0030	0.0016	0.0001	98.5%
Trans depth (mm)	0.3324	−0.0706	−0.0424	0.0019	−0.0029	0.0096	−0.0008	−0.0004	0.0008	−0.0003	0.0008	99.9%
Plastic work (% of lnit K.E.)	45.9609	0.1951	−0.2899	0.2672	0.3157	−0.0161	1.1800	0.0945	−0.1580	−0.0518	0.0909	97.8%

Table 12 Response data and fit quality for Rc60-300M stochastic Rel-YS simulations

Std normal Z-score	Rel-YS (MPa)	σ_x at surf (MPa)	σ_x min (MPa)	Depth at min (mm)	Trans depth (mm)	Plastic work percent of original K.E.
−2.5	464	457	−1604	0.091	0.227	40.06%
−1.25	588	406	−1652	0.091	0.231	43.72%
0	711	337	−1680	0.102	0.234	46.95%
1.25	835	279	−1730	0.102	0.236	49.69%
2.5	958	200	−1742	0.102	0.239	52.18%
Normal dist R^2		99.51%	97.11%	75.00%	99.61%	99.37%
Std error estimate		51.4	27.5	——	0.002	2.42%

exception of the surface residual stress (σ_x), the standard errors for the Rc60 shot are significantly less than those for the Rc45 shot, thereby suggestive of a process than can be better controlled.

VI. Summary and Conclusions

A comprehensive investigation into the influence of process parameters on the residual stress state produced in a 4340M (300M) high-strength steel target by a single impact was conducted using a nonlinear transient dynamic finite element model as a simulation backbone. Two accepted shot specifications were considered with one nominally 15% softer (Rc45) and the other nominally 15% harder (Rc60) than the 300M target material (nominally Rc52). An experimental 2^4 factorial design matrix was used to detect the significance of four process parameters including shot diameter (0.72 vs 1.08 mm), shot velocity (50 vs 75 mps), target thickness (1.44 vs 2.88 mm) and the presence of friction (frictionless contact vs $\mu = 0.5$) on five residual stress response variables. The five response variables included the residual stress (σ_x) at the target surface, residual stress (σ_x) at the profile minimum, depth corresponding to the profile minimum residual stress (σ_x), depth at the core transition from compression to tension, and the plastic work done on the target as a percentage of the original shot kinetic energy. Because the geometry was axisymmetric (i.e., sphere impacting the flat end of a cylinder) all references to σ_x actually refer to the radial component of stress at the bottom of the dent caused by the impact. While this was the component of stress that was of primary interest, there was also limited interest in the σ_y normal component of stress due to the fact that the effect of friction was being investigated as well as whether or not the particle was experiencing local yielding after impact. For each of the five responses a set of 10 coefficients (four main effect and six 2-factor interaction) was evaluated to form a generalized linear model (GLM) that would predict the nominal response of a given combination of process parameters. In addition, the effect of the relative hardness between the particular shot used and the 300M target was considered as a probabilistic source of residual error to the deterministic response results predicted by the GLM. A review of the completed results leads to the following observations:

1) The Rc45 shot leaves a *puddle* of residual tension in the target at the base of the imposed dent regardless of the combination of process parameters. Obviously, a region of tension would exacerbate fatigue crack growth, however, it is expected that the shower of media in an actual shot-peening process would eliminate this small tensile region given the degree of overlap in coverage and the tendency toward homogeneity in the resulting residual stress state across the entire

surface.

2) The Rc60 shot leaves a puddle of residual compression in the target at the base of the imposed dent for frictionless contact regardless of the combination of the other process parameters, however, the corresponding cases with friction produce a puddle of residual tension similar in magnitude to those for the Rc45 shot. Again, the small region of residual tension seen in these cases would not be likely to occur in an actual shot-peening process due to the overlap in coverage and homogeneity of the resulting residual stress state.

3) In all cases the Rc45 shot particle suffers significant plastic deformation in the form of a flattened edge whereas the Rc60 shot particle maintains its rounded shape while sustaining little or no plastic deformation.

4) The (subsurface) minimum compressive residual stress (σ_x) mean for the Rc60 shot is −1670 MPa (Table 11) which is nearly twice the mean of −960 MPa for the Rc45 shot (Table 8).

5) The minimum residual stress (σ_x) GLM fit quality, as demonstrated by its coefficient of simple determination (R^2), for the Rc60 shot is 98.0% with significant diameter, velocity, and friction main effects (Table 11) and a significant interaction between diameter and velocity vs 89.9% for the Rc45 shot where the only significant main effect is velocity and there are no significant interactions (Table 8).

6) The mean depth at the minimum residual stress (σ_x) is 0.1265 mm with (a GLM) R^2 of 98.7% for the Rc45 shot (Table 8) vs 0.1403 mm with an R^2 of 98.8% for the Rc60 shot (Table 11). Keeping in mind that the residual stress profile continues in compression until the transition depth is reached, it is conservative to use this depth as a criterion for the maximum depth wherein cracks would be arrested. Nonetheless, if such a criterion is used, a surface crack depth of between 0.1265 and 0.1403 mm, which is in line with the size of an initial quality flaw, would be arrested. An actual shot-peening process would likely see this depth along with the transition depth increased due to work hardening from the multitude of shot impacts.

7) The mean transition depth (near-surface compression to core tension) is 0.2667 mm for the Rc45 shot (Table 8) vs 0.3324 mm for the Rc60 shot (Table 11), both with a GLM R^2 of 99.9%. Specifically, the transition depth on average is about 25% greater for the Rc60 vs Rc45 shot. Keep in mind that the transition depth ranges (when all 16 runs are considered) were between 0.178 and 0.355 mm for the Rc45 shot and between 0.216 and 0.463 mm for the Rc60 shot.

8) The target plastic work (percent of initial particle kinetic energy) is 12.23% with an R^2 of 71.9% for the Rc45 shot (Table 8) vs 45.9% with an R^2 of 97.8% for the Rc60 shot (Table 11).

9) For the Rc45 data in Table 6, there is a relationship between the plastic work and the minimum residual stress (σ_x) with the correlation being −0.304; there is also a 0.147 correlation between plastic work and the residual stress (σ_x) at the surface.

10) For the Rc60 data in Table 10, there is a very modest relationship between the plastic work and the minimum residual stress (σ_x) with the correlation being 0.083; there is also a −0.234 correlation between plastic work and the residual stress σ_x at the surface. The reason the ratio of the plastic work to minimum residual stress (σ_x) correlation is much weaker for the Rc60 than for the Rc45 is likely due to the much harder surface being impacted.

11) Given the rather weak relationships established in items 9) and 10), it must be pointed out that there is a very strong relationship between the amount of plastic work and the magnitude of the minimum residual stress (σ_x) when any given condition from Table 6 is compared with the corresponding condition in Table 10. Obviously, if more plastic work can be done then a much higher minimum residual stress (σ_x) will result.

12) The standard error estimates made from an assumed normal distribution of the relative yield strength of the shot vs target are significantly lower for the Rc60 shot (Table 12) and the fit quality is better vs the corresponding values for the Rc45 shot (Table 9).

Given these observations, one can conclude that use of the hard Rc60 shot delivers a more desirable residual stress state while at the same time offering a significantly more manageable process from a quality control standpoint. This overall finding is not at all unexpected given that it is common knowledge among practitioners (e.g., [12]) and end users of shot peening technology. This finding is explainable by the physics of the shot impingement. Because the Rc60 shot is 15% harder than the target vs 15% softer for the Rc45 shot, the Rc60 is able to convert significantly more of its kinetic energy into target plastic work and thereby produce a greater depth and magnitude of compressive residual stress. The additional plastic work, greater depth of compressive residual stress penetration and magnitude of compressive residual stress are all desirable effects of a shot-peening process. It is important to keep in mind that the findings of this investigation are applicable to a single shot impact and, as such, do not provide a direct correlation to a real shot-peening process (i.e., no effect of overlap and work hardening from the shower of media). However, with regard to the plastic work done on the target and the depth and magnitude of the compressive residual stress for Rc45 vs Rc60 shot, the trend of the findings is expected to be similar to an actual shot-peening process.

References

[1] "SAE (1952/1983) Procedure for Using Standard Shot-Peening Test Strip, SAE Standard J443," *SAE Handbook*, Vol. 1, SAE International, Warrendale, PA, Approved 1952, Revised 1983, Sec. 9.

[2] Zion, H. L., "A Dynamic Finite Element Simulation of the Shot-Peening Process," Ph.D. Dissertation, Mechanical Engineering Department, Georgia Institute of Technology, 2003.

[3] Dowling, N. E., *Mechanical Behavior of Materials*, Prentice–Hall, Englewood Cliffs, NJ, 1993, pp. 182–185.

[4] *Metallic Materials and Elements for Aerospace Vehicle Structures*, Vol. 1, MIL-HDBK-5H, U.S. Dept. of Defense, Washington, DC, Dec. 1998, p. 2 22.

[5] *ASM Metals Handbook*, 9th ed., Vol. 2, American Society for Metals International, Metals Park, OH, 1978, pp. 425–429.

[6] Box, G. E. P., Hunter, W. G., and Hunter, J. S., *Statistics for Experimenters*, Wiley, New York, 1978.

[7] Kobayashi, M., Matsui, T., and Murakami, Y., "Mechanism of Creation of Compressive Residual Stress by Shot Peening," *International Journal of Fatigue*, Vol. 20, No. 5, 1998, pp. 351–357.

[8] Cook, R. D., Malkus, D. S., and Plesha, M. E., *Concepts and Applications of Finite Element Analysis*, 3rd ed., Wiley, New York, 1989, pp. 395–418.

[9] *ANSYS Structural Analysis Guide 001245*, 5th ed., SAS IP, Inc., Houston, PA, Nov. 1999, pp. 8–32.

[10] Box, G. E. P., Hunter, W. G., and Hunter, J. S., *Statistics for Experimenters*, Wiley, NY, 1978, pp. 327–332.

[11] Box, G. E. P., Hunter, W. G., and Hunter, J. S., *Statistics for Experimenters*, Wiley, NY, 1978, pp. 322–323.

[12] *Shot Peening Applications*, 7th ed., Metal Improvement Company, Inc., Paramus, NJ, 1991.

A. Palazotto
Associate Editor